Available online at www.eccomasproceedia.org
Eccomas Proceedia SMART (2023) 2027-2037

ECCOMAS
Proceedia

X ECCOMAS Thematic Conference on Smart Structures and Materials
SMART 2023
D.A. Saravanos, A. Benjeddou, N. Chrysochoidis and T. Theodosiou (Eds)

ENHANCED ELECTROMECHANICAL COUPLING OF PIEZOELECTRIC BEAMS THROUGH AN INNOVATIVE DESIGN

D. GIBUS[*], P. GASNIER[†], A. MOREL[*], O. FREYCHET[†] AND A. BADEL[*]

[*] SYMME, Université Savoie Mont-Blanc
F-74000 Annecy, France
e-mail: David.Gibus@univ-smb.fr

[†] Université Grenoble Alpes, CEA, LETI, MINATEC
F-38000 Grenoble, France

Abstract. This paper reports the finite element model simulations of an innovative design of piezoelectric cantilevers in order to maximize their global electromechanical coupling coefficient k^2.
A strong electromechanical coupling coefficient is necessary for piezoelectric cantilever to improve their performances as vibration energy harvesters. Its value can be increased by minimizing the strain in the width direction of the beam.
The purpose of the proposed design is to block the lateral deformations of the beam while allowing longitudinal deformations. This is implemented by placing several rigid bars on the piezoelectric patches in the width direction. By using finite element model simulations, we show that the coupling coefficient of a PMN-PT based cantilever is multiplied by 1.89 when using steel lateral bars (from k^2=21.3 % to k^2=40.3 %).
Such a design is interesting when strong global electromechanical coupling coefficients are needed for resonant frequency tuning by electrical methods, or to increase the performance of lead-free materials that are still weakly coupled materials.

Key words: Piezoelectricity, cantilever, mechanical design, electromechanical coupling, vibration energy harvesting, finite element model simulations.

1 INTRODUCTION

Vibration energy harvesting is an interesting approach to powering autonomous sensor nodes. Among the solutions, piezoelectric cantilevers are often preferred because their resonant frequencies can be easily adjusted to a given value of the ambient vibration frequency and they are easy to produce. Among the design considerations, maximising the electromechanical coupling coefficient $k^2$is one of the most critical parameters. Indeed, maximise k^2 is necessary to maximise the power harvested for weakly coupled cantilevers and maximizing k^2 improves the tunability of the resonant frequency by electrical methods for strongly coupled cantilevers [1]. Several electrical methods and implementations have already been proposed to tune the resonant frequency of piezoelectric vibration energy harvester. Maximizing the coupling

Peer-review under responsibility of the organizing committee of SMART 2023.
doi: 10.7712/150123.9971.445167

coefficient of cantilever k^2 can be performed by using piezoelectric materials with strong coupling coefficients k_{31}^2 and optimizing the mechanical design of the devices .

Design solutions have already been proposed in the literature and mainly concern the optimisation of geometrical parameters [1]–[3]. Recently, it has been shown that maximising the beam width/length ratio for piezoelectric ceramic cantilevers maximises the coupling coefficient. Indeed, when piezoelectric ceramics are used, the coupling coefficient of cantilevers is maximised when the lateral deformations are minimisedin the beam [1]. For this reason, wide ceramic-based beams with small width deformations have a much better coupling coefficient than narrow ceramic-based beams. As the design of wide beams increases the complexity of the design when the overall volume is constrained, a solution to limit the lateral deformations of narrow beams would be relevant.

In this paper, we propose an innovative design to improve the coupling coefficient of narrow beams. The aim of the design is to block lateral deformations while allowing longitudinal deformations in order to obtain a high coupling coefficient with a reduced space requirement. This is achieved by placing multiple rigid bars on the piezoelectric patches in the width direction of the beam. The next section introduces the parameters of a common piezoelectric cantilever and the material consideration for narrow and wide beams. Section 3 introduces the design innovation and demonstrates its interest to maximize the coupling coefficient for an example configuration using Comsol simulations. The last section discusses the impact of the geometrical parameters of the bars on the improvement of the coupling coefficients.

2 WIDTH CONSIDERATION FOR COMMON CANTILEVER

This section presents the proposed device and discusses the impact of material parameters and beam width/length ratio on the global coupling coefficient of the cantilever. The constitutive equations of piezoelectricity are derived to determine the equivalent coupling coefficient of piezoelectric materials under the assumptions of plane strain and plane stress.

The studied cantilever is a piezoelectric bimorph with a proof mass (Figure 1). The two piezoelectric layers and the substrate have the same length (L_b) and the same width (B). As it has been shown as optimal configuration [1], the piezoelectric layers are entirely covered with electrodes and their thicknesses are noted h_p.

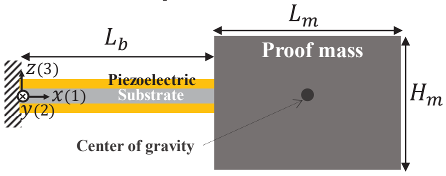

Figure 1: Piezoelectric cantilever with proof mass

The linear constitutive relations of piezoelectricity are described in equation (1) using Kevin-Voigt notation. Where $\boldsymbol{E}$, $\boldsymbol{S}$, $\boldsymbol{D}$ and $\boldsymbol{T}$ are the vectors of the electric field, strain, electric displacement and stress respectively. The superscript $(\,)^t$ denotes transpose. $\boldsymbol{e}$ is the piezoelectric constant matrix, $\boldsymbol{\epsilon^S}$ is the dielectric matrix at constant strain, $\boldsymbol{c^E}$ is the elastic stiffness matrix of the piezoelectric material at null electric field.

$$\begin{pmatrix} \boldsymbol{T} \\ \boldsymbol{D} \end{pmatrix} = \begin{bmatrix} \boldsymbol{c^E} & -\boldsymbol{e^t} \\ \boldsymbol{e} & \boldsymbol{\varepsilon^S} \end{bmatrix} \begin{pmatrix} \boldsymbol{S} \\ \boldsymbol{E} \end{pmatrix} \tag{1}$$

Because of the electrodes disposition, the displacement field $\boldsymbol{D}$ and the electric field $\boldsymbol{E}$ are only considered in the transverse direction ($\boldsymbol{D} = D_3\vec{\boldsymbol{z}}$ and $\boldsymbol{E} = E_3\vec{\boldsymbol{z}}$).

For the beam modeling, the stress is assumed to be zero in the *z* direction and one of the two following assumptions has to be considered for the out-of-plane stress:

(i) plane stress assumption is used for narrow beams (*B*/*Lb* < 0.2) for which no stress is considered ($T_2 = 0$) in the out-of-plane direction (*Oy* in Figure 1)

(ii) plane strain assumption is used for wide beams (*B*/*Lb* > 5) for which no strain is considered ($S_2 = 0$) in the out-of-plane direction.

We therefore express the in-plane piezoelectric constitutive equations (2) and (3) .

$$\begin{cases} T_1^p = c_{11}^{ef} S_1 - e_{31}^{ef} E_3 & (2) \\ D_3 = e_{31}^{ef} S_1 + \epsilon_{33}^{ef} E_3 & (3) \end{cases}$$

T_1^p, D_3, E_3 are the longitudinal stress, the transverse displacement field and the transverse electric field respectively. c_{11}^{ef}, e_{31}^{ef}, ϵ_{33}^{ef} are the effective piezoelectric coefficients according to the given plane stress or plane strain consideration. The piezoelectric effective coefficients are deduced from the piezoelectric matrix $\boldsymbol{d}$, the compliance matrix $\boldsymbol{s^E}$ and the free dielectric matrix $\boldsymbol{\epsilon^T}$ (with $\boldsymbol{e} = \boldsymbol{d}\boldsymbol{s^E}^{-1}$, $\boldsymbol{c^E} = \boldsymbol{s^E}^{-1}$ and $\boldsymbol{\epsilon^S} = \boldsymbol{\epsilon^T} - \boldsymbol{d}\boldsymbol{s^E}^{-1}\boldsymbol{d^t}$) in equations (4) to (6).

$$c_{11}^{ef} = \begin{cases} \dfrac{1}{s_{11}^E} & \text{plane stress} \\ \dfrac{s_{22}^E}{s_{22}^E s_{11}^E - {s_{12}^E}^2} & \text{plane strain} \end{cases} \tag{4}$$

$$e_{31}^{ef} = \begin{cases} \dfrac{d_{31}}{s_{11}^E} & \text{plane stress} \\ \dfrac{s_{22}^E d_{31} - d_{32} s_{12}^E}{s_{22}^E s_{11}^E - {s_{12}^E}^2} & \text{plane strain} \end{cases} \tag{5}$$

$$\epsilon_{33}^{ef} = \begin{cases} \epsilon_{33}^T - \dfrac{d_{31}^2}{s_{11}^E} & \text{plane stress} \\ \epsilon_{33}^T + \dfrac{s_{22}^E d_{31}^2 - 2\, d_{31} d_{32} s_{12}^E + s_{11}^E d_{32}^2}{{s_{12}^E}^2 - s_{11}^E s_{22}^E} & \text{plane strain} \end{cases} \tag{6}$$

The electromechanical coupling coefficient of the piezoelectric material k_{31}^2 depends on the effective piezoelectric coefficients e_{31}^{ef}, c_{11}^{ef} and ϵ_{33}^T and vary according to the plane stress or plane strain assumption. k_{31}^2 is expressed in equation (7) [1].

$$k_{31}^2 = \frac{e_{31}^{ef}}{c_{11}^{ef}\epsilon_{33}^{ef} + e_{31}^{ef}} \tag{7}$$

We can thus define ${k_{31}^{l}}^2$ as the electromechanical coupling coefficient corresponding to the plane stress assumption and ${k_{31}^{w}}^2$ as the electromechanical coupling coefficient corresponding to the plane strain assumption. They are expressed in (8) and (9) respectively from the equation (7) and equations (4) to (6). The values of ${k_{31}^{l}}^2$ and ${k_{31}^{w}}^2$ are provided for examples of piezoelectric materials in Table 1.

$${k_{31}^{l}}^2 = \frac{d_{31}^2}{\varepsilon_{33}^T s_{11}^E} \tag{8}$$

$${k_{31}^{w}}^2 = \frac{\left(d_{31} - \frac{s_{12}^E}{s_{22}^E} d_{32}\right)^2}{\left(\varepsilon_{33}^T - \frac{d_{32}^2}{s_{22}^E}\right)\left(s_{11}^E - \frac{{s_{12}^E}^2}{s_{22}^E}\right)} \tag{9}$$

Table 1: Material coupling coefficient of example piezoelectric materials

	Plane stress	Plane strain
	${k_{31}^{l}}^2$	${k_{31}^{w}}^2$
TRS X2B [001] Single crystal PMN-29PT [4]	19.6%	68.1%
Noliac NCE51 Ceramic PZT-5A [5]	15.1%	34.3%
Microfine* [6] Single crystal PZN-PT 5.5% [011]	81.0%	60.0%

*${k_{32}^{l}}^2$ and ${k_{32}^{w}}^2$ are given for PZN-PT [011]

Most piezoelectric materials, such as ceramics and [001] axis-polarized PMN-PT and PZN-PT single crystals, have a higher mode 31 coupling coefficient in the plane strain configuration, while others, such as [011] axis-polarized PMN-PT and PZN-PT, have a higher coupling coefficient in the plane stress configuration. Therefore, we need to design wide beams for the former class and narrow beams for the latter if we wish to maximize the overall coupling coefficient. These propensities depend on crystal classes and polarization directions.

Due to their symmetry, piezoelectric ceramics have higher coupling coefficients for wide beams than for narrow beams. Indeed, piezoelectric ceramics belong to the ∞m class of crystals [7, p. 12]. For this configuration, the coupling coefficient considered in plane strain ${k_{31}^{w}}^2$ can be expressed by equation (10) as a function of the coupling coefficient considered in plane stress ${k_{31}^{l}}^2$. ν_p is a coefficient equivalent to Poisson's ratio given in (11).

$$k_{31}^{w\,2} = \frac{k_{31}^{l\,2}}{1-k_{31}^{l\,2}} \frac{\left(1+\nu_p\right)^2}{1-\nu_p^2} \quad (10) \qquad \nu_p = -\frac{s_{12}^E}{s_{11}^E} \quad (11)$$

Since ν_p is always positive and less than 1 for ceramics, equation (10) shows that $k_{31}^{w\,2}$ is always greater than $k_{31}^{l\,2}$ for ceramics. Equation (10) is also true for 4mm and 6mm class materials when axes 1 and 3 of the piezoelectric material correspond to the O_x and O_z axes of the cantilever, respectively.

However, the design of wide beams can be problematic if devices with small volumes and low resonant frequencies are required. Indeed, the desired B/L_b ratio should be higher than 5 to satisfy the assumption of plane deformation. Moreover, the length of the beam L_b is often maximized to reduce the resonance frequency. Therefore, following these design guidelines, a harvester corresponding to the plane deformation condition and having a low resonant frequency would require having a large length L_b and a very large width B. Therefore, a compromise for the beam width/length ratio must usually be found during the design.

3 INNOVATIVE DESIGN

3.1 Presentation of the innovation

In this section, we propose a method to improve the coupling coefficient of beams of small width. The goal here is to block lateral deformations while allowing longitudinal deformations in order to obtain a high coupling coefficient with a reduced space requirement (small width). This is implemented by placing several rigid bars on the piezoelectric patches in the width direction. Figure 2.a. shows a common cantilever and Figure 2.b an enhanced version with the addition of bars. The geometric parameters of the bars are defined in Figure 3.

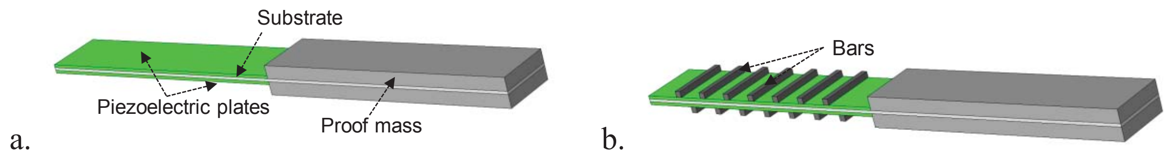

Figure 2: a. Common cantilever, b. Enhanced cantilever with bars

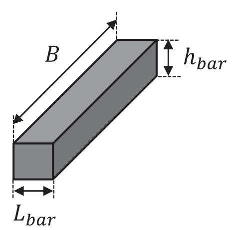

Figure 3: Bars geometric parameters

The fabrication can be done by gluing the bars on an existing piezoelectric beam. As discussed in the next section, the bars must be wide enough to be rigid (L_{bar} must be large enough) and thin enough not to prevent the beam from deforming in the longitudinal direction (the value of L_{bar} must not be too large). The bars are placed on the piezoelectric materials on both sides of the beam.

The improvement of the coupling depends on:
- The initial cantilever:
  - Coupling coefficients ${k_{31}^{l}}^2$ and ${k_{31}^{w}}^2$ of the piezoelectric material,
  - The stiffness of the piezoelectric material and the substrate
  - The geometry (length of the beam, mass and thickness of the piezoelectric materials and the substrate)
- The bars:
  - Dimensions (height h_{bar}, length L_{bar})
  - The stiffness of the material of the bars
  - Number and arrangement (distance between each bar, staggered or face to face arrangement)

3.2 Example

We propose to estimate the impact of the bars to the coupling coefficient by 3-dimensional finite element simulations using Comsol Multiphysics modal analysis on an example. The initial system is the PMN-PT based cantilever that was studied in a previous paper [1] whose dimensions are defined in Table 2.

Table 2 : Properties of the example cantilever

Piezoelectric material	PMN-29PT [001] TRS X2B
Substrate material	Steel
Beam length L_b	45mm
Masse length L_m	45mm
Mass height H_m	5mm
Substrate thickness h_s	0.5mm
Piezoelectric thickness h_p	0.5mm
Beam and mass width B	10mm

The distributions of the longitudinal and lateral deformations are given in Figure 4 and Figure 5. A second simulation is performed in which 14 steel bars of dimensions 1×1×10mm (7 on each side of the beam) are added as shown in Figure 2.b. For this simulation, the bars are considered perfectly fixed to the piezoelectric material. The longitudinal and lateral strain distributions are given in Figure 6 and Figure 7. From the simulations, it can be seen that the longitudinal strains are preserved between the basic system and the system with bars (Figure 4 to Figure 8) while the lateral strains are reduced. The short circuit resonance frequency (f_{sc}) and the open circuit resonance frequency (f_{oc}) are used to calculate the coupling and are given on the right of the figures with equation (12). The short-circuit resonance frequency is slightly influenced by the addition of bars while the coupling coefficient is increased by more than 75% compared to the basic cantilever.

Table 3 : Example of the influence of the addition of side bars on the coupling coefficient and the resonant frequency simulated by Comsol Multiphysics

Without bars

Figure 4: Longitudinal strain S_1 of the initial cantilever seen from above

Figure 5: Lateral strain S_2 of the initial cantilever seen from above

$f_{sc} = 33.0\text{Hz}$
$f_{oc} = 37.2\text{Hz}$
$\boldsymbol{k^2 = 21.3\%}$

With bars

Figure 6: Longitudinal strain S_1 of the enhanced cantilever seen from above

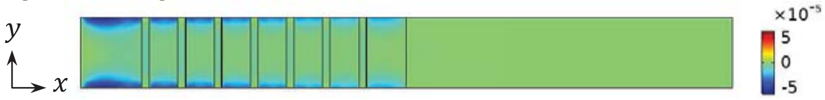

Figure 7: Lateral strain S_2 of the enhanced cantilever seen from above

$f_{sc} = 38.3\text{Hz}$
$f_{oc} = 48.5\text{Hz}$
$\boldsymbol{k^2 = 37.7\%}$

$$k^2 = \frac{f_{oc}^2 - f_{sc}^2}{f_{oc}^2} \tag{12}$$

Figure 8 depictsts the longitudinal and lateral strains S_1 and S_2 at the centre of the upper piezoelectric patch for a displacement of 0.1 mm at the tip end of the beam (at $x = L_b$). While the lateral strain is significantly reduced, the longitudinal strain is not much affected. Decreasing the lateral deformation tends toward the plane strain assumption and causes the global electromechanical coupling coefficient k^2 to tend toward ${k_{31}^{w}}^2$. Moreover, as having a homogeneous longitudinal distribution of S_1 improves k^2 in cantilevers [1], maintaining a good longitudinal distribution despite the bars maximizes the coupling.

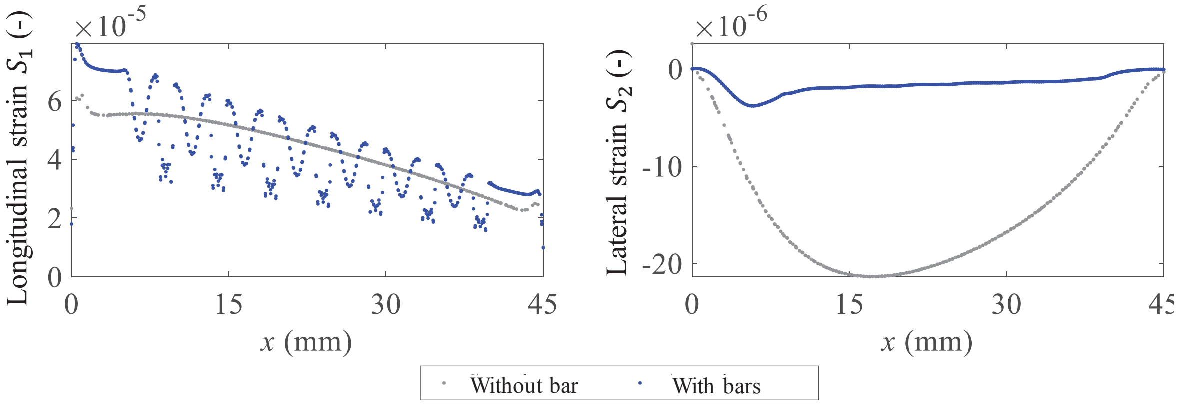

Figure 8: Longitudinal strain S_1 on the left and lateral strain S_2 on the right simulated by Comsol 3D at the centre of the upper piezoelectric patch for a tip displacement of 0.1mm at $x = L_b$

For simplicity of assembly, the number of bars can be limited and an improvement of the coupling is still possible. For example, the coupling coefficient is increased by 25% if only 2 bars are used (1 on each side of the beam). The optimal dimensions of the bars depend on their number.

The addition of bars allows a significant increase in the coupling associated with simplicity of manufacture, all in a reduced space since it is not necessary to have a structure of large width.

4 PARAMETRIC STUDY OF THE INFLUENCE OF THE BARS

From the basic initial cantilever, we propose to analyze the influence of the geometrical and material parameters of the bars through a parametric analysis by modal analysis with Comsol Multiphysics. We keep the same beam configuration and the same number of bars: 7 on each side (14 bars in total). In this analysis, we vary the dimensions and the Young's modulus of the bars.

Table 4 : Configurations of the bars tested in simulation

Bars Young modulus Y_b (GPa)	[4 ; 20 ; 200]
Height of the bars h_{bar} (mm)	[0.25 ; 0.5 ; 1 ; 2.5 ; 5]
Length of the bars L_{bar} (mm)	[0.5 ; 1 ; 2.5 ; 5]

It is proposed to analyse the evolution of the coupling coefficient as a function of the size ratios according to the thickness e_H and according to the length e_L expressed in (13) and (14) where n_{bar} is the number of bars. e_H represents the ratio between the thickness of the bars and the thickness of the base beam comprising the substrate and the piezoelectric patches. e_L

represents the ratio between the length of the beam on which bars are arranged and the total length of the beam.

$$e_H = h_{bar}/(h_s + 2h_p) \quad (13) \qquad e_L = n_{bar}L_{bar}/L_b \quad (14)$$

The coupling coefficients of the initial cantilever, denoted k_{init}^2, and the harvester with bars, denoted k_{bar}^2, are calculated from the short-circuit and open-circuit resonance frequencies. The relative variation of the coupling coefficient $(k_{bar}^2 - k_{init}^2)/k_{init}^2$ is given in Figure 9 as a function of e_H and e_L.

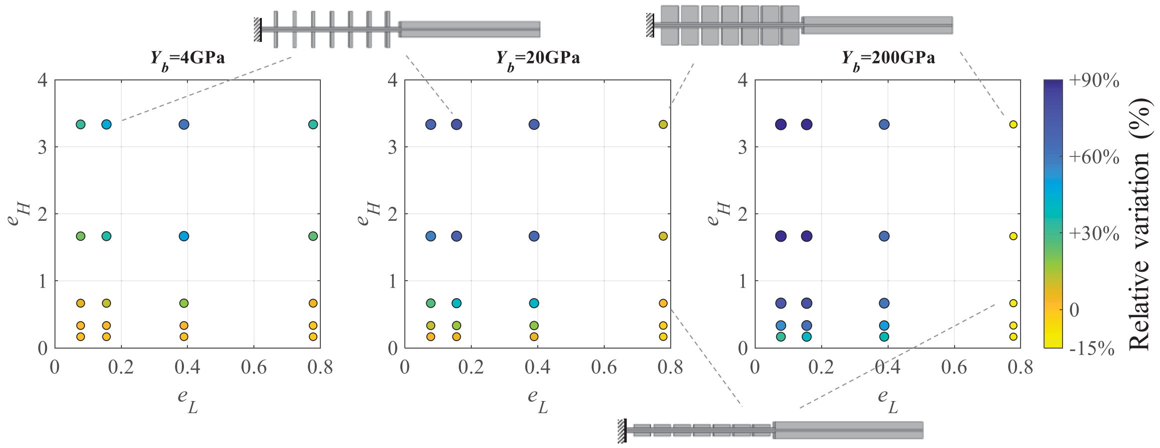

Figure 9: Variation of the coupling coefficient $(k_{bar}^2 - k_{init}^2)/k_{init}^2$ generated by the addition of bars as a function of the length ratio e_L and the thickness ratio e_H

It can be seen that the more rigid the material of the bars, the more influence the bars have on the harvester. Therefore, adding 14 bars of dimensions (L_{bar}; h_{bar}) = (1mm;5mm) allow a relative increase of 89% of the coupling coefficient for steel (Y_b=200 GPa) while the increase is respectively 78% and 47% for Young's modulus Y_b of 20 GPa and 4 GPa for the same dimensions. However, a rigid material can lead to a significant reduction in the coupling coefficient :for (L_{bar}; h_{bar})= (5mm;5mm) and Y_b=200 GPa, the bars cause an 11% decrease in the coupling coefficient while these dimensions cause a 33% increase for Y_b=4 GPa. Therefore, we find that the bars must be sufficiently rigid to block the lateral deformations. The bars must also be narrow enough to avoid blocking longitudinal deformations.

We propose to analyze the variation of the coupling as a function of a coefficient equivalent to the bending stiffness of the bars. As the bending stiffness of a beam depends on the cube of its thickness, the coefficient $Y_b h_{bar}^3$ seems interesting to express the influence of the height of the bars on the bending stiffness of the beam. Figure 10 shows the variation of coupling as a function of the ratio $Y_b h_{bar}^3/YI$ for different values of e_L , where YI is the bending stiffness of the base beam.

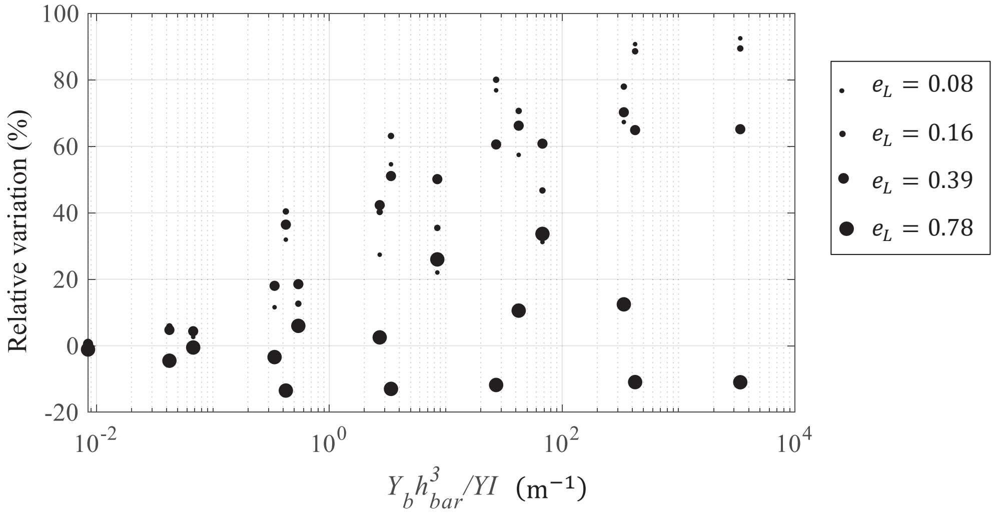

Figure 10: Variation of coupling coefficient k^2 as a function of the ratio of equivalent bending stiffnesses for several length ratios e_L. The size of the points represents the value of e_L

We note that the larger $Y_b h_{bar}^3$ is, the more impact the addition of the bars has on the global coupling coefficient. For our harvester, the addition of bars has a significant impact on the coupling coefficient when $Y_b h_{bar}^3/YI > 0.1$ m^{-1}. When e_L is small, the impact is positive (increasing the coupling coefficient) and when e_L is large, the impact can be negative. For our configurations, the coupling coefficient is always increased when the bars cover less than 40% of the total length of the beam. The optimal configuration corresponds to thin and stiff bars because the product $n_{bar}L_{bar}$ is small and the product $Y_b h_{bar}^3$ is large.

Design guidelines can be deduced from 3D simulations. A study for various initial cantilever configuration (various thicknesses, beam length, substrate material and piezoelectric material for example) still need to be performed. Furthermore, an experimental validation of the increase of the electromechanical coupling coefficient has to be done.

5 CONCLUSION

Our work introduced innovative design that improve the global electromechanical coupling coefficient k^2 of piezoelectric cantilevers.

The electromechanical coupling of piezoelectric cantilevers can be improved by minimizing the deformations according to the beam width. This effect is possible by increasing the width of the cantilever, to respect to the plane strain assumption. However, compacity problems quickly arise as the size of energy harvesting devices is usually limited.

The innovative design consists in placing several rigid bars on the piezoelectric patches in the width direction, to block the lateral deformations of cantilever while allowing longitudinal deformations. By using Comsol Multiphysics simulations, we show several configurations that increase the coupling while others can have a detrimental effect (i.e., decrease of k^2). The size and material of the bars have to be judiciously chosen.

We have shown that the addition of laterally arranged bars on a piezoelectric beam can significantly increase the coupling coefficient through 3D finite element simulations. Indeed k^2 is multiplied by 1.89 (from k^2=21.34 % to k^2=40.3 %) for a PMN-PT based cantilever when using 14 steel lateral bars

Such a design is interesting when high values of k^2 are required to improve the tunability of the resonant frequency by electrical methods, or to increase the harvested power by cantilevers using lead-free materials. The feasibility of this solution has yet to be demonstrated experimentally.

REFERENCES

[1] D. Gibus *et al.*, 'Strongly coupled piezoelectric cantilevers for broadband vibration energy harvesting', *Applied Energy*, vol. 277, p. 115518, Nov. 2020, doi: 10.1016/j.apenergy.2020.115518.

[2] J. Ducarne, O. Thomas, and J.-F. Deü, 'Placement and dimension optimization of shunted piezoelectric patches for vibration reduction', *Journal of Sound and Vibration*, vol. 331, no. 14, pp 3286-3303, Jul. 2012, doi: 10.1016/j.jsv.2012.03.002.

[3] Q.-M. Wang, X.-H. Du, B. Xu, and L. E. Cross, 'Electromechanical coupling and output efficiency of piezoelectric bending actuators', *IEEE transactions on ultrasonics, ferroelectrics, and frequency control*, vol. 46, no. 3, pp 638-646, 1999.

[4] 'TRS Technologies, Inc.', *http://www.trstechnologies.com/Resources*. http://www.trstechnologies.com/Resources (accessed Sep. 19, 2018).

[5] 'Noliac piezoceramic material NCE51', *Noliac - Your Piezo Partner*. http://www.noliac.com/products/materials/nce51/ (accessed Oct. 16, 2019).

[6] S. Zhang and L. C. Lim, 'Property matrices of [011]-poled rhombohedral Pb(Zn1/3Nb2/3)O3–(4.5-7)%PbTiO3 single crystals', *AIP Advances*, vol. 8, no. 11, p. 115010, Nov. 2018, doi: 10.1063/1.5064418.

[7] J. Erhart, P. Půlpán, and M. Pustka, *Piezoelectric Ceramic Resonators*. in Topics in Mining, Metallurgy and Materials Engineering. Cham: Springer International Publishing, 2017. doi: 10.1007/978-3-319-42481-1.